Online Supporting Information

for

"Mitochondrial Transcription Factor A Binds to and Promotes Mutagenic Transcriptional Bypass of O^4-Alkylthymidine Lesions"

Xiaomei He, Pengcheng Wang and Yinsheng Wang*

Department of Chemistry, University of California Riverside, CA 92521-0403, USA

*To whom correspondence should be addressed: yinsheng.wang@ucr.edu

Table of Contents

Supplementary Experimental Conditions

Data Analysis

The above LC-MS/MS data were searched using Maxquant (Version 1.2.2.5)[1] against UniProt human proteome database (UP000005640), to which contaminants and reverse sequences were added. The maximum number of missed cleavages for trypsin was two per peptide. Cysteine carbamidomethylation and methionine oxidation were set as fixed and variable modifications, respectively. MaxQuant multiplicity was set to 2, and [$^{13}C_6$]-L-arginine and [$^{13}C_6$,$^{15}N_2$]-L-lysine were selected as heavy amino acids. The search was performed with the tolerances in mass accuracy of 10 ppm and 20 ppm for MS and MS/MS, respectively. The required false-positive discovery rate was set at 1% at both the peptide and protein levels, with the minimal required peptide length being 6 amino acids. The match between runs option was used, with the alignment window and minimum protein ratio counts being 5 min and 1.0, respectively.

Western Blot

Protein samples were separated on a 10% SDS-PAGE gel and transferred to a nitrocellulose membrane (Bio-Rad). After blocking with blotting-grade blocker (Bio-Rad), the membrane was incubated in PBS-T buffer (PBS with 0.1% Tween 20) containing primary antibody and 5% BSA for 2 h, and then incubated with the HRP-conjugated secondary antibody in a 5% blotting-grade blocker. After thorough washing of the membrane with PBS-T, the signal was detected with ECL Western blotting detection reagent (Amersham). Primary antibodies used in this study included DDB1 (Santa Cruz Biotechnology, sc-376860; 1:1000), DDB2 (Santa Cruz Biotechnology, sc-81246; 1:1000), TFAM (Santa Cruz Biotechnology, sc-376672; 1:1000) and HMGB2 (Santa Cruz

Biotechnology, sc-271689; 1:1000).

Generation of Recombinant TFAM Proteins

The construct for producing recombinant GST-His-TFAM was prepared by PCR amplification of the *TFAM* gene from a cDNA library with primers containing BamHI and XhoI restriction recognition sites. The digested PCR product was ligated into pGEX-4T1 vector and the successful incorporation of the TFAM coding sequence was confirmed by Sanger sequencing. For truncated TFAM proteins, the corresponding coding sequences (i.e. HMG-box A: 43-118 aa; HMG-box B: 150-219 aa) were amplified by PCR and inserted into the pGEX-4T1 vector using the same method.

The pGEX-TFAM plasmid was transformed into competent Rosetta (DE3) pLysS *Escherichia coli* cells and TFAM expression was induced by 1 mM isopropyl 1-thio-*β*-D-galactopyranoside (IPTG, Sigma) at 37°C for 4 h. The cells were subsequently harvested by centrifugation. The cell pellets were then lysed by sonication in a 10-mL buffer containing 50 mM Tris (pH 7.5), 0.5 M NaCl, 10% (*v/v*) glycerol, a protease inhibitor cocktail (Roche), and 1 mM phenylmethylsulfonyl fluoride (PMSF, Sigma). The cell lysate was then centrifuged at 10,000 g for 15 min. The recombinant proteins were purified by using Glutathione Superflow Agarose (Pierce) and, if needed, purified again using TALON Metal Affinity Resin. The purities of the resulting proteins were confirmed by SDS-PAGE analyses, and their quantities determined by Quick Start Bradford Protein Assay kit (Bio-Rad). The proteins were used immediately or stored at -80°C until use.

Electrophoretic Mobility Shift Assay (EMSA)

EMSA was performed using a previously reported method with some modifications.[2] Briefly, various amounts of purified GST-TFAM were incubated with 10 fmol ^{32}P-labeled control or

lesion-containing 20-mer DNA substrates in a buffer containing 10 mM Tris-HCl (pH 7.5), 100 mM KCl, 1 mM EDTA, 0.1 mM DTT, 10 μg/mL BSA, and 10% glycerol. The mixtures were incubated at room temperature for 30 min and then resolved at 4°C on an 8% native polyacrylamide gel containing 40 mM Tris-acetate (pH 8.0) and 2 mM EDTA. Electrophoresis was performed at 200 V for 50 min and the labeled DNA probes and their protein-bound complexes were detected using a Typhoon PhosphorImager (GE). The data were processed using ImageJ (NIH). The K_d values were calculated using GraphPad Prism 5 with non-linear regression for curve fitting using a one-binding-site model.

References:

1. Cox, J.; Mann, M., MaxQuant enables high peptide identification rates, individualized p.p.b.-range mass accuracies and proteome-wide protein quantification. *Nat. Biotechnol.* **2008,** *26*, 1367.
2. Hellman, L. M.; Fried, M. G., Electrophoretic mobility shift assay (EMSA) for detecting protein–nucleic acid interactions. *Nat. Protoc.* **2007,** *2*, 1849.

Table S1. A list of candidate O^2-*n*BudT-binding proteins identified from SILAC-based quantitative proteomic experiments. Listed are the protein ratios (O^2-*n*BudT/dT) obtained from three forward (Fwd) and three reverse (Rvs) SILAC labeling experiments. "NaN" indicates that the protein was not quantified in the specific experiment.

Protein Names	Gene Names	Ratio Fwd-1	Ratio Fwd-2	Ratio Fwd-3	Ratio Rvs-1	Ratio Rvs-2	Ratio Rvs-3	Ave. Ratio	S.D.
Nucleolar and coiled-body phosphoprotein 1	NOLC1	NaN	4.8	4.4	NaN	2.8	NaN	4.0	1.1
RNA-binding protein FUS	FUS	NaN	4.3	NaN	2.7	NaN	NaN	3.5	1.1
TATA-box-binding protein	TBP	3.3	NaN	NaN	NaN	2.0	NaN	2.7	0.9
Nuclear cap-binding protein subunit 1	NCBP1	3.0	2.5	2.4	3.9	2.3	1.7	2.7	0.7
THO complex subunit 2	THOC2	NaN	4.8	3.3	1.9	1.3	2.1	2.7	1.4
Pre-mRNA-processing factor 40 homolog A	PRPF40A	NaN	3.8	3.1	2.4	1.6	1.3	2.4	1.1
Serine/arginine-rich splicing factor 6	SRSF6	NaN	1.9	1.7	NaN	3.6	NaN	2.4	1.0
Treacle protein	TCOF1	NaN	1.8	NaN	3.8	1.3	NaN	2.3	1.3
Non-histone chromosomal protein HMG-17	HMGN2	0.8	4.3	1.3	2.2	NaN	NaN	2.2	1.6
Dynamin-2	DNM2	1.4	3.4	1.9	1.6	2.0	2.2	2.1	0.7
DNA damage-binding protein 1	DDB1	1.8	2.6	1.3	2.0	1.5	2.8	2.0	0.6
Sister chromatid cohesion protein PDS5 homolog A	PDS5A	1.9	2.3	1.8	1.8	2.7	1.6	2.0	0.4
E3 ubiquitin-protein ligase	UHRF2	NaN	1.5	2.7	1.8	NaN	NaN	2.0	0.6
Splicing factor 3B subunit 1	SF3B1	2.0	2.1	1.7	1.9	2.0	1.3	1.8	0.3
DNA topoisomerase 1	TOP1	1.0	2.6	1.8	1.7	1.8	1.9	1.8	0.5
Leucine-rich PPR motif-containing protein, mitochondrial	LRPPRC	1.2	2.4	2.1	2.2	1.6	1.2	1.8	0.5
DNA-dependent protein kinase catalytic subunit	PRKDC	NaN	2.1	NaN	NaN	1.6	NaN	1.8	0.3

Protein Names	Gene Names	Ratio Fwd-1	Ratio Fwd-2	Ratio Fwd-3	Ratio Rvs-1	Ratio Rvs-2	Ratio Rvs-3	Ave. Ratio	S.D.
DNA damage-binding protein 2	DDB2	2.5	1.6	1.4	1.9	1.5	NaN	1.8	0.4
RNA-binding protein 25	RBM25	NaN	1.5	NaN	NaN	2.2	1.5	1.7	0.4
Heterogeneous nuclear ribonucleoprotein F	HNRNPF	1.9	1.9	1.4	2.3	0.9	1.3	1.6	0.5
DNA mismatch repair protein Msh6	MSH6	NaN	1.5	1.7	NaN	1.7	1.6	1.6	0.1

Table S2. A list of candidate O^4-*n*BudT-binding proteins. Listed are the protein ratios (O^4-*n*BudT/dT) obtained from three forward (Fwd) and three reverse (Rvs) SILAC labeling experiments. "NaN" indicates that the protein was not quantified in the specific experiment.

Protein Names	Gene Names	Ratio Fwd-1	Ratio Fwd-2	Ratio Fwd-3	Ratio Rvs-1	Ratio Rvs-2	Ratio Rvs-3	Ave. Ratio	S.D.
Transcription factor A, mitochondrial	TFAM	3.7	4.5	4.6	17.9	5.6	6.7	7.2	5.4
Spectrin beta chain, non-erythrocytic 5	SPTBN5	0	0	18.7	7.6	2.8	12.7	7.0	7.5
Thymocyte nuclear protein 1	THYN1	NaN	NaN	4.6	6.3	3.7	4.0	4.7	1.2
Serine/threonine-protein phosphatase 2A 65 kDa regulatory subunit A alpha isoform	PPP2R1A	NaN	4.6	5.4	6.2	1.9	NaN	4.5	1.9
60S ribosomal protein L34	RPL34	2.6	1.0	2.2	18.6	1.8	0.9	4.5	6.9
60S ribosomal protein L23a	RPL23A	3.4	1.0	1.4	17.6	2.6	1.0	4.5	6.5
DNA replication licensing factor MCM5	MCM5	NaN	1.7	2.3	10.7	NaN	1.3	4.0	4.5
High mobility group protein B1	HMGB1	4.7	3.0	4.8	2.4	2.0	5.0	3.7	1.3
NADH dehydrogenase [ubiquinone] 1 beta subcomplex subunit 6	NDUFB6	NaN	NaN	1.7	9.5	1.9	0.9	3.5	4.0
60S ribosomal protein L37a	RPL37A	2.8	1.0	2.1	12.2	1.9	0.9	3.5	4.3
Sister chromatid cohesion protein PDS5 homolog A	PDS5A	4.6	2.7	6.2	2.7	1.0	2.8	3.4	1.8
Myosin light chain 1/3, skeletal muscle isoform	MYL1	4.5	NaN	1.8	8.1	1.7	0.7	3.4	3.0
60S ribosomal protein L4	RPL4	3.9	1.6	2.5	8.1	2.0	1.2	3.2	2.6
Voltage-dependent anion-selective channel protein 1	VDAC1	NaN	1.1	3.0	9.1	1.5	0.8	3.1	3.5
THO complex subunit 2	THOC2	1.0	3.6	5.9	3.5	2.3	2.0	3.0	1.7
Receptor of activated protein C kinase 1	RACK1	NaN	3.1	3.3	NaN	NaN	2.4	3.0	0.5
40S ribosomal protein S6	RPS6	4.8	1.2	2.4	5.9	2.4	1.2	3.0	2.0
Cytochrome b-c1 complex subunit 6, mitochondrial	UQCRH	NaN	7.1	2.2	3.1	1.3	1.0	2.9	2.5

Protein Names	Gene Names	Ratio Fwd-1	Ratio Fwd-2	Ratio Fwd-3	Ratio Rvs-1	Ratio Rvs-2	Ratio Rvs-3	Ave. Ratio	S.D.
Serine/arginine-rich-splicing factor 11	SRSF11	NaN	2.1	3.0	6.6	1.3	1.7	2.9	2.1
Cullin-associated NEDD8-dissociated protein 1	CAND1	NaN	2.3	1.3	3.1	NaN	4.8	2.9	1.5
HUMAN TATA-binding protein-associated factor 2N	TAF15	1.7	6.9	1.6	3.3	1.7	1.7	2.8	2.1
Serine/threonine-protein kinase	VRK1	1.9	1.2	3.7	5.7	1.5	NaN	2.8	1.9
ATP synthase subunit alpha, mitochondrial	ATP5F1A	NaN	1.9	1.1	9.4	0.7	0.9	2.8	3.7
60S ribosomal protein L8	RPL8	2.3	1.2	2.3	6.3	3.4	1.2	2.8	1.9
NADH dehydrogenase [ubiquinone] 1 beta subcomplex subunit 8, mitochondrial	NDUFB8	4.5	NaN	1.5	4.4	1.2	1.9	2.7	1.6
Inhibitor of growth protein	ING1	3.2	0.6	1.6	7.7	2.0	1.1	2.7	2.6
Regulation of nuclear pre-mRNA domain-containing protein 2	RPRD2	NaN	3.0	NaN	3.6	1.4	NaN	2.6	1.1
Gamma-tubulin complex component	TUBGCP2	NaN	1.9	NaN	4.3	1.6	NaN	2.6	1.5
Ras-related protein Rab-1B	RAB1B	NaN	2.6	NaN	2.4	NaN	NaN	2.5	0.1
DNA topoisomerase 1	TOP1	3.4	1.0	2.6	4.5	2.0	1.3	2.5	1.3
Proliferation marker protein Ki-67	MKI67	2.7	1.6	1.7	4.3	3.2	1.2	2.5	1.2
Pre-mRNA-processing factor 40 homolog A	PRPF40A	NaN	3.2	2.9	NaN	1.3	2.1	2.4	0.9
Histone H3	HIST2H3PS2	4.3	NaN	NaN	3.8	0.8	0.7	2.4	2.0
Ubiquitin-associated protein 2-like	UBAP2L	3.1	NaN	0.7	3.5	1.3	3.5	2.4	1.4
Luc7-like protein 3	LUC7L3	NaN	2.9	NaN	2.6	1.3	NaN	2.3	0.8
Talin-1	TLN1	NaN	2.9	NaN	3.6	0.6	NaN	2.3	1.6
T-complex protein 1 subunit delta	CCT4	NaN	2.8	NaN	1.8	NaN	NaN	2.3	0.7
Tyrosine-protein kinase BAZ1B	BAZ1B	NaN	1.0	2.5	4.6	0.8	2.7	2.3	1.5

Protein Names	Gene Names	Ratio Fwd-1	Ratio Fwd-2	Ratio Fwd-3	Ratio Rvs-1	Ratio Rvs-2	Ratio Rvs-3	Ave. Ratio	S.D.
ATP synthase subunit d, mitochondrial	ATP5H	NaN	0.7	4.1	4.8	0.7	1.1	2.3	2.0
High mobility group protein B2	HMGB2	2.7	NaN	1.3	1.3	NaN	3.8	2.3	1.2
Transformer-2 protein homolog beta	TRA2B	NaN	2.6	NaN	1.8	NaN	NaN	2.2	0.6
ATP synthase subunit beta, mitochondrial	ATP5F1B	NaN	2.5	NaN	1.8	NaN	NaN	2.2	0.6
Y-box-binding protein 3	YBX3	2.1	NaN	NaN	NaN	NaN	2.3	2.2	0.1
60S ribosomal protein L14	RPL14	2.8	1.0	2.4	4.0	2.1	1.1	2.2	1.1
Ribosomal L1 domain-containing protein 1	RSL1D1	2.2	0.9	2.4	4.1	2.4	1.1	2.2	1.2
Condensin complex subunit 1	NCAPD2	NaN	2.5	NaN	5.2	0.3	0.4	2.1	2.3
CDGSH iron-sulfur domain-containing protein 1	CISD1	NaN	NaN	2.3	4.0	1.0	1.1	2.1	1.4
Guanine nucleotide-binding protein-like 3	GNL3	NaN	3.3	1.3	2.6	1.0	2.2	2.1	0.9
RNA cytidine acetyltransferase	NAT10	NaN	2.7	2.4	1.7	1.6	2.2	2.1	0.5
60S ribosomal protein L18a	RPL18A	2.5	1.2	1.9	3.9	1.8	1.0	2.1	1
Nucleolar protein 14	NOP14	1.5	NaN	NaN	1.8	2.8	2.1	2.1	0.6
Homeobox protein OTX1	OTX1	NaN	2.0	2.4	2.9	0.8	NaN	2.0	0.9
cAMP-responsive element modulator	CREM	1.3	1.6	2.2	4.2	1.1	1.4	2.0	1.1
Splicing factor 3B subunit 1	SF3B1	1.1	2.6	2.1	2.7	1.6	1.7	2.0	0.6
Elongin-A	ELOA	1.5	NaN	NaN	2.5	NaN	NaN	2.0	0.6
Importin subunit beta-1	KPNB1	NaN	2.6	NaN	1.2	1.4	2.5	1.9	0.7
GTPase Kras	KRAS	NaN	1.4	2.5	2.1	1.8	1.7	1.9	0.4
Cleavage and polyadenylation-specificity factor subunit 7	CPSF7	NaN	1.7	2.0	4.1	0.7	0.9	1.9	1.4
Signal recognition particle 14 kDa protein	SRP14	3.8	0.9	1.1	3.3	1.5	1.1	1.9	1.3
Protein LYRIC	MTDH	1.5	1.5	1.6	3.8	1.5	1.0	1.8	1.0
RRP12-like protein	RRP12	2.3	NaN	NaN	2.3	1.5	1.0	1.8	0.7
U4/U6 small nuclear ribonucleoprotein Prp3	PRPF3	0.4	4.8	0.8	2.7	1.0	1.0	1.8	1.7

Protein Names	Gene Names	Ratio Fwd-1	Ratio Fwd-2	Ratio Fwd-3	Ratio Rvs-1	Ratio Rvs-2	Ratio Rvs-3	Ave. Ratio	S.D.
Annexin A1	ANXA1	NaN	1.8	NaN	1.2	3.8	0.5	1.8	1.4
60S ribosomal protein L9	RPL9	1.8	1.0	1.9	4.1	1.3	0.9	1.8	1.2
Eukaryotic translation initiation factor 4 gamma 1	EIF4G1	NaN	1.7	2.4	2.6	1.0	1.1	1.7	0.7
Splicing factor U2AF 65 kDa subunit	U2AF2	1.6	1.4	1.6	2.4	1.5	1.8	1.7	0.3
Poly(rC)-binding protein 2	PCBP2	1.4	1.9	2.3	2.2	0.9	1.7	1.7	0.5
Peptidyl-tRNA hydrolase 2, mitochondrial	PTRH2	NaN	1.2	2.3	3.6	1.0	0.7	1.7	1.2
ATP-binding cassette sub-family F member 1	ABCF1	NaN	1.5	1.9	1.8	NaN	NaN	1.7	0.2
Nuclear pore glycoprotein p62	NUP62	NaN	1.7	NaN	2.7	0.7	NaN	1.7	1.0
TAR DNA-binding protein 43	TARDBP	NaN	2.3	1.0	3.5	0.9	1.0	1.7	1.1
General transcription factor IIF subunit 1	GTF2F1	NaN	NaN	1.6	NaN	1.8	NaN	1.7	0.1
NADH-ubiquinone oxidoreductase 75 kDa subunit, mitochondrial	NDUFS1	NaN	0.9	2.2	1.6	NaN	NaN	1.6	0.6
2,3-cyclic-nucleotide 3-phosphodiesteras	CNP	NaN	1.3	1.7	NaN	1.6	NaN	1.5	0.2

Figure S1. Negative-ion ESI-MS and MS/MS for the characterizations of d(ATGGCGXGCTATGATCCTAT), X = O^2-*n*BudT: (a) Negative-ion ESI-MS; (b) the product-ion spectrum of the $[M-6H]^{6-}$ ion (*m/z* 1028.7).

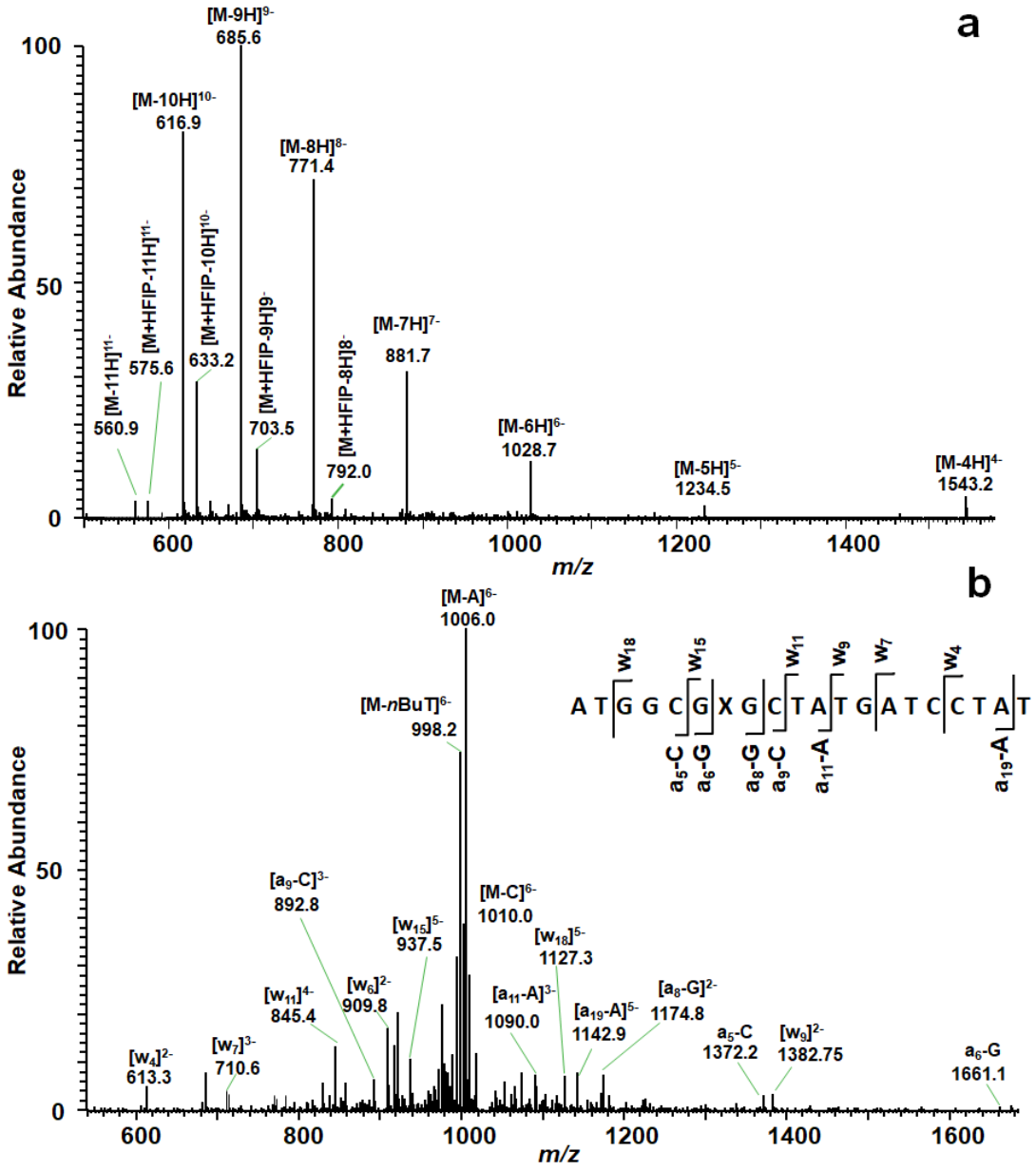

Figure S2. Negative-ion ESI-MS and MS/MS for the characterizations of d(ATGGCGXGCTATGATCCTAT), X = O^4-*n*BudT: (a) Negative-ion ESI-MS; (b) the product-ion spectrum of the $[M-6H]^{6-}$ ion (*m/z* 1028.8).

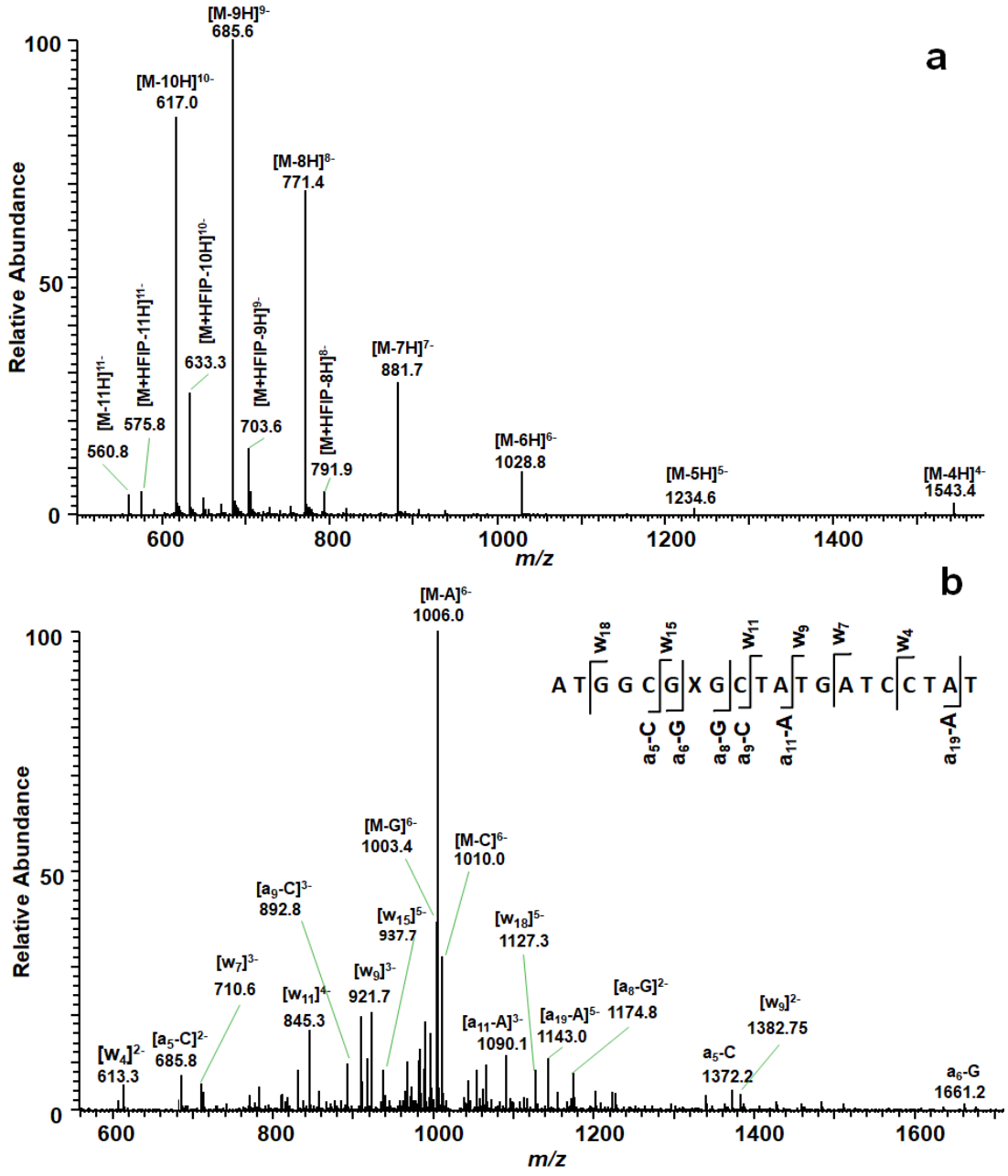

Figure S3. Negative-ion ESI-MS and MS/MS for the characterizations of d(ATGGCGXGCTATGATCCTAT), X = O^4-POBdT: (a) Negative-ion ESI-MS; (b) the product-ion spectrum of the $[M-6H]^{6-}$ ion (*m/z* 1043.9).

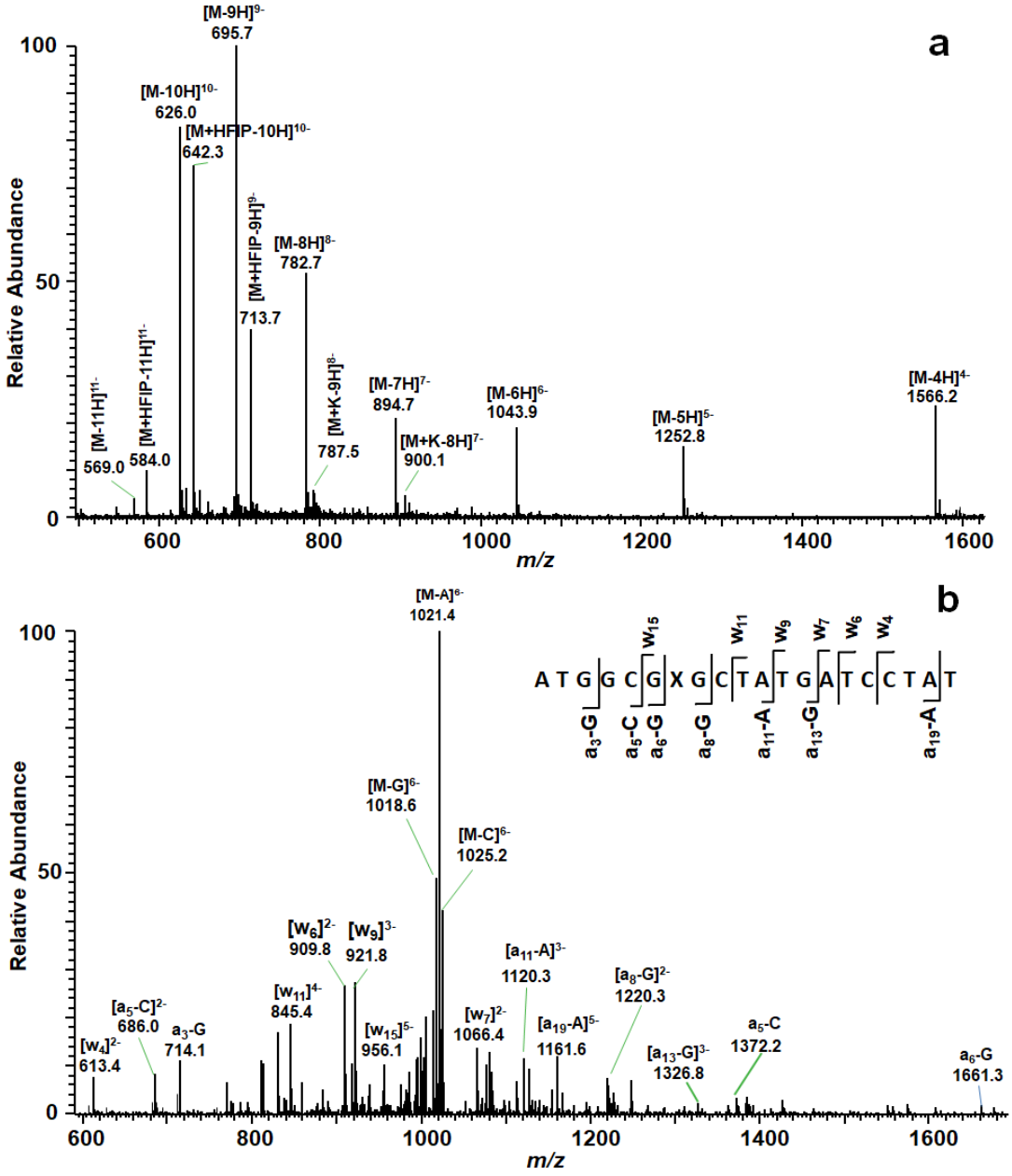

Figure S4. Representative PAGE gel image for assessing the purity of the synthesized oligodeoxyribonucleotides.

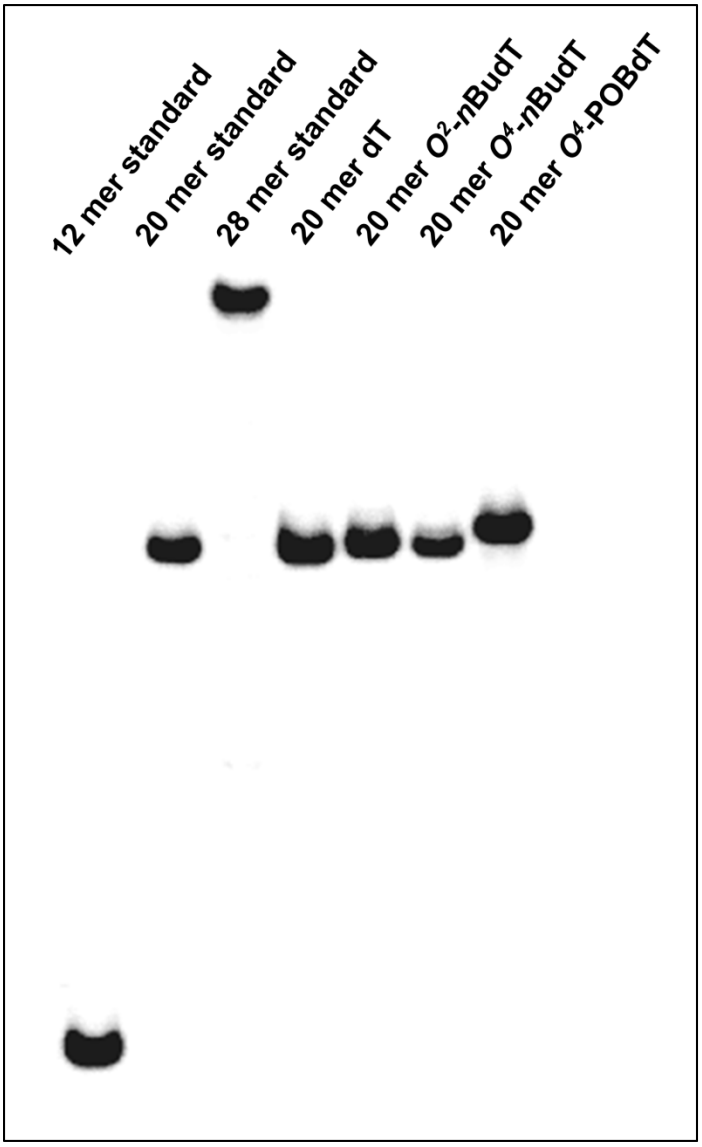

Figure S5. A scatter plot showing the proteins identified from pull-down assays using O^2-*n*BudT-containing DNA relative to the corresponding lesion-free DNA with nuclear protein lysates isolated from HeLa cells.

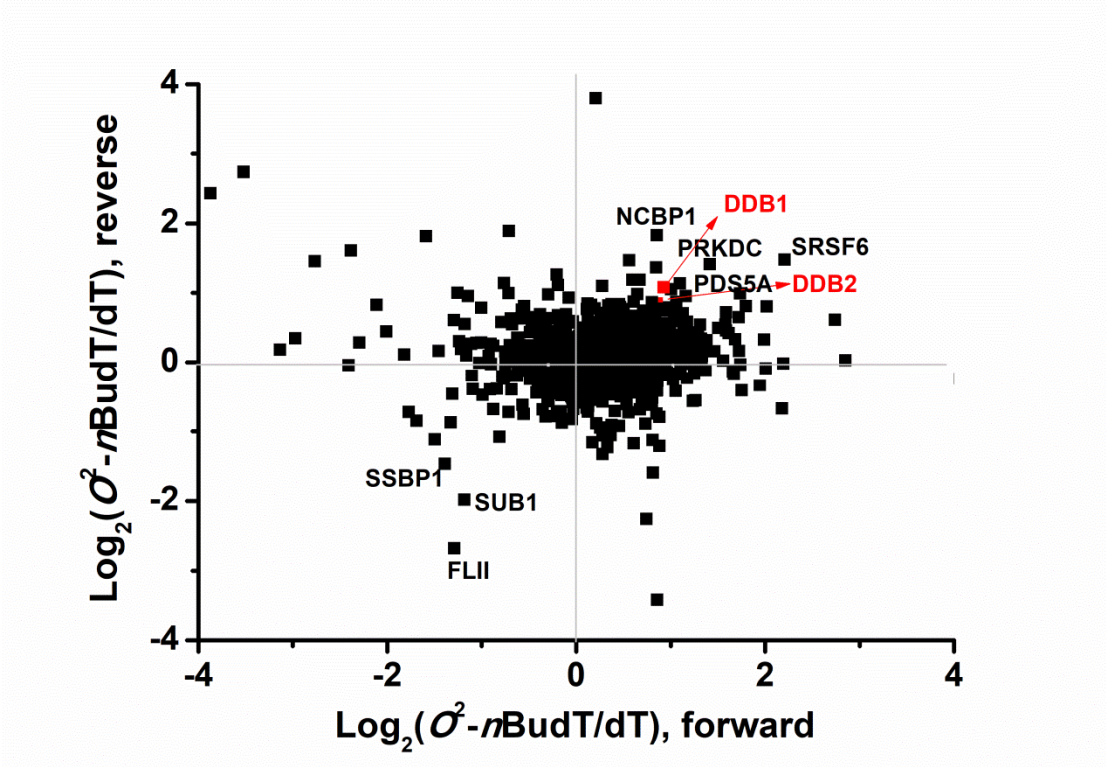

Figure S6. ESI-MS/MS of the $[M + 2H]^{2+}$ ions of light (a) and heavy (b) arginine-containing peptide, EMLGGEIIPR, derived from DDB1.

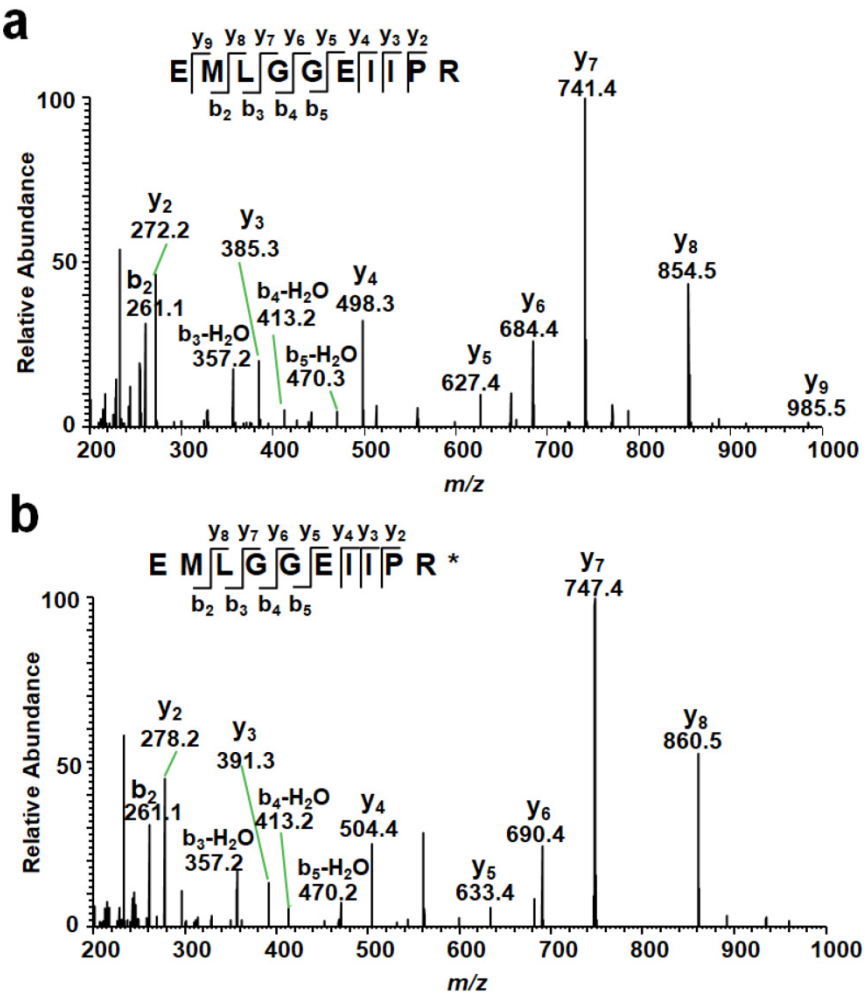

Figure S7. ESI-MS/MS of the $[M + 2H]^{2+}$ ions of light (a) and heavy (b) lysine-containing peptide, FNPLNTNQFYASSMEGTTR, derived from DDB2.

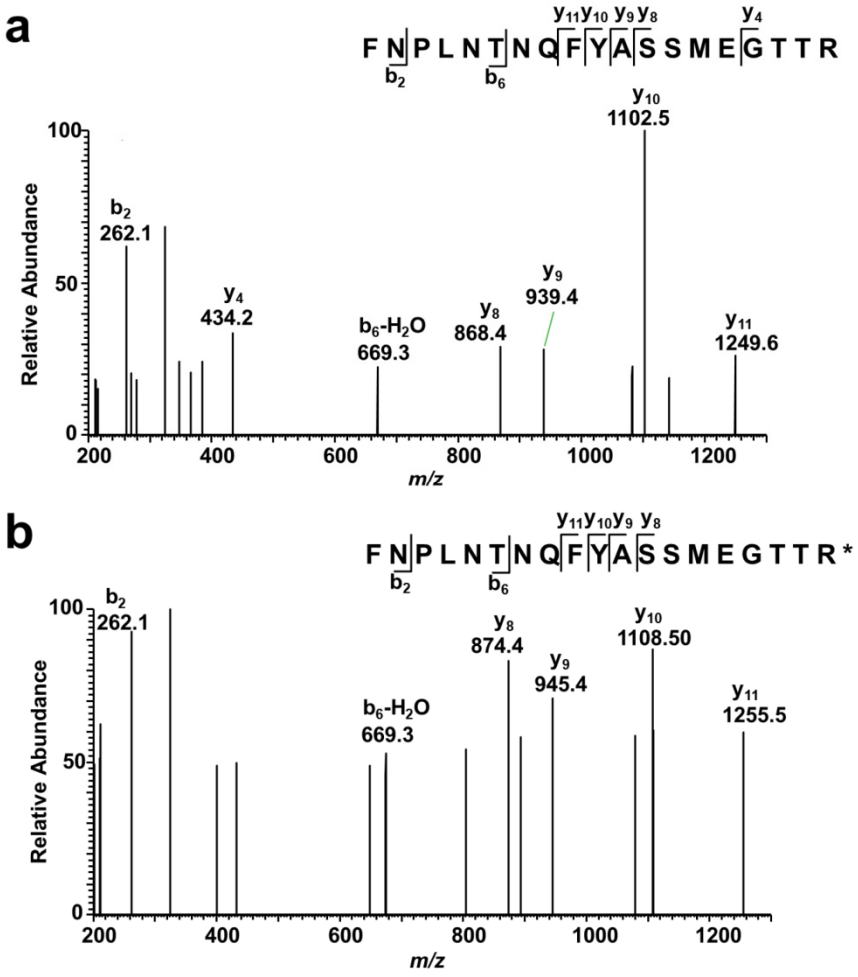

Figure S8. ESI-MS/MS of the $[M + 2H]^{2+}$ ions of light (a) and heavy (b) lysine-containing peptide, FKEQLTPSQIMSLEK, derived from TFAM.

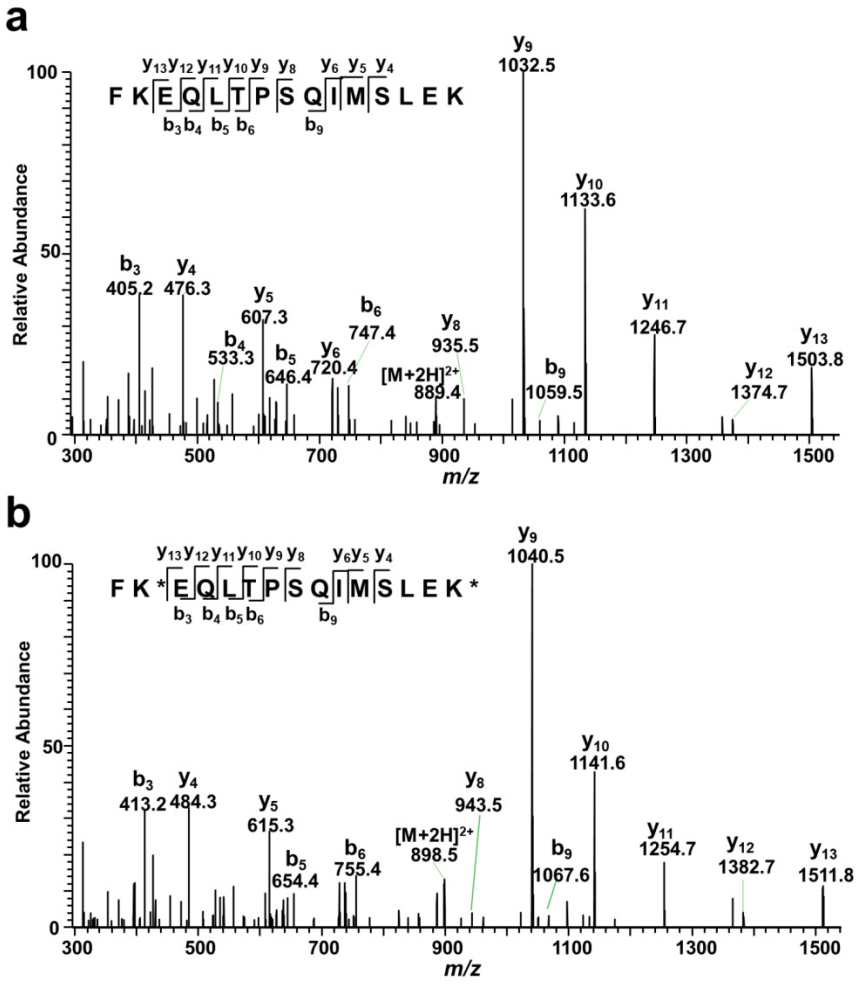

Figure S9. Representative ESI-MS (a, b) and ESI-MS/MS (c, d) of the $[M + 2H]^{2+}$ ions of light and heavy arginine-containing peptide, AEWQVYKEEISR, derived from TFAM.

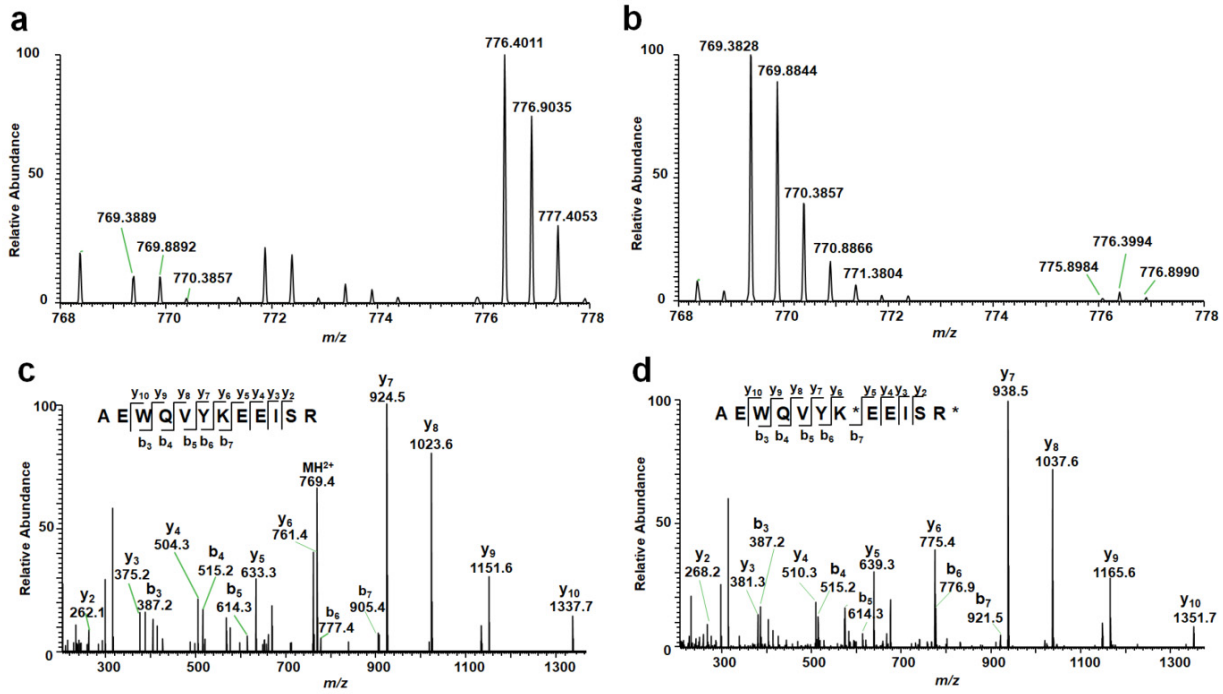

Figure S10. SDS-PAGE for monitoring the purification of recombinant full-length TFAM protein. The gel was stained with Coomassie blue.

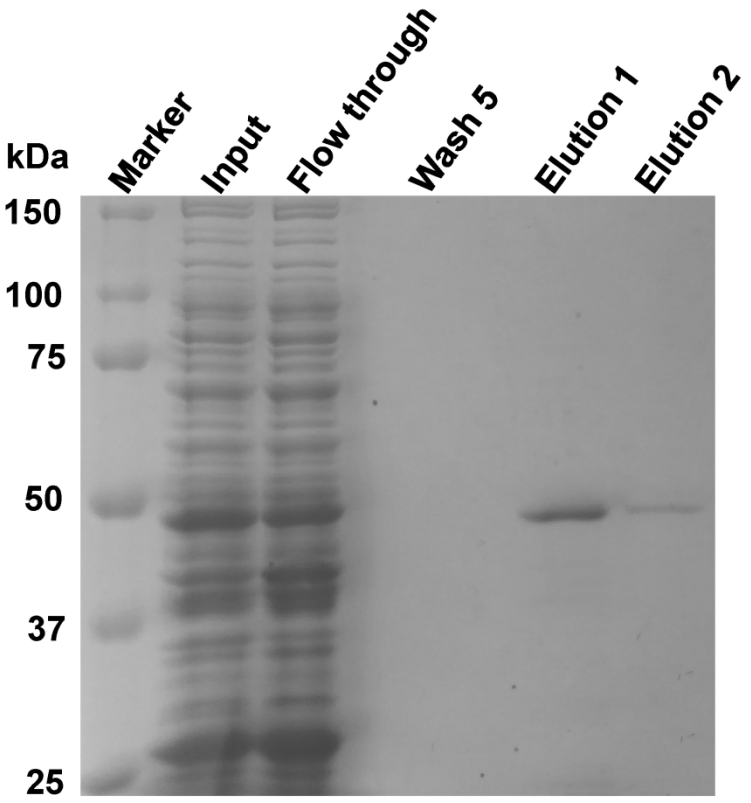

Figure S11. (a) A schematic diagram illustrating the domain structure of TFAM protein. (b) SDS-PAGE gel for monitoring the purifications of truncated forms of recombinant TFAM protein that contain only the HMG-box A or HMG-box B domains (i.e. TFAM-HMG-box A and TFAM-HMG-box B).

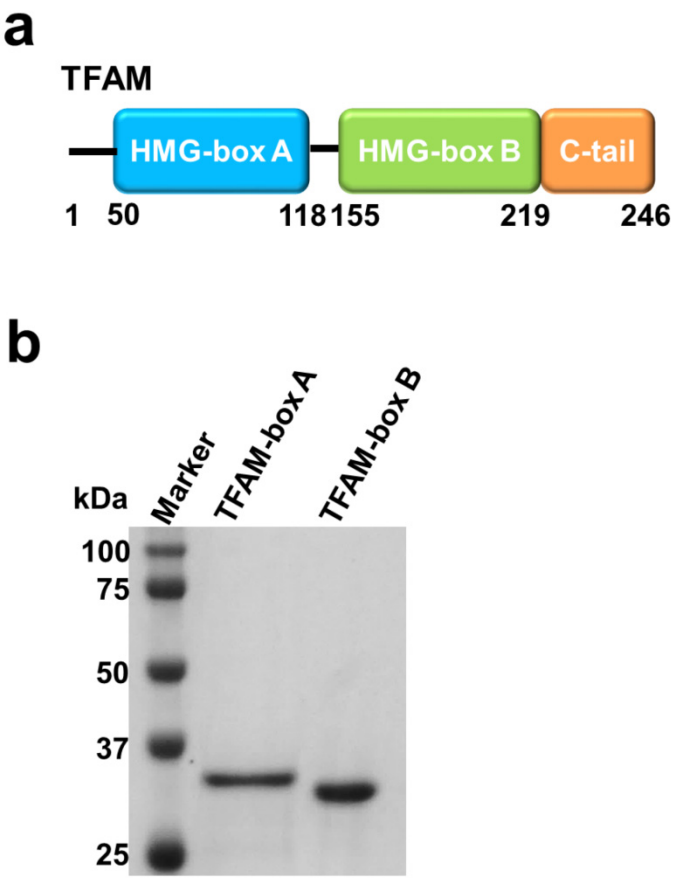

Figure S12. EMSA for measuring the binding affinities of HMG-box A (a) and HMG-box B (b) domains of TFAM with lesion-free and O^4-alkyldT DNA probes (n = 3). Error bars represent S. D.

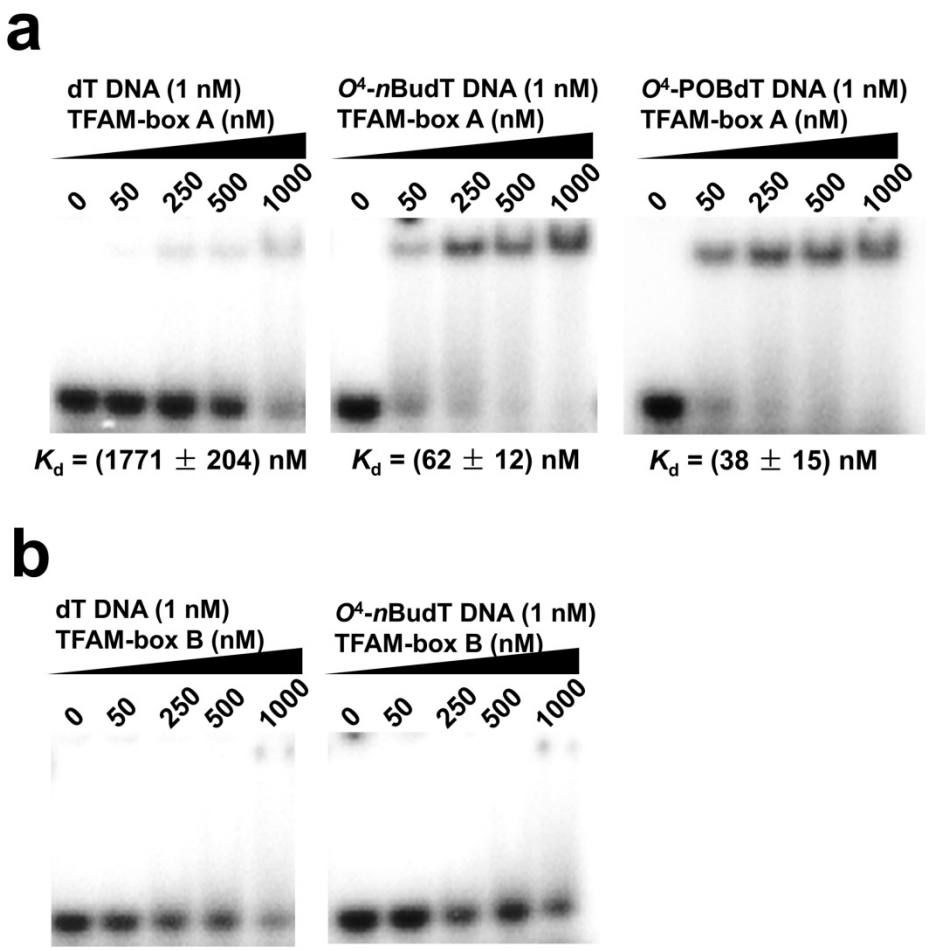

Figure S13. Representative ESI-MS results showing the detection of the $[M-3H]^{3-}$ ions of restriction fragments of interest arising from the hRNAPII-mediated transcription of O^2-*n*BudT- (a, b), O^4-*n*BudT- (c) or O^4-POBdT-bearing substrates (d). '13mer A' represents the non-mutagenic product, i.e., d(AATTATAGCACGC), whereas '13mer T' and '13mer G' designate the corresponding products carrying an A→U or A→G mutation opposite the lesion site, i.e., d(AATTATAGCTCGC) and d(AATTATAGCGCGC), respectively.

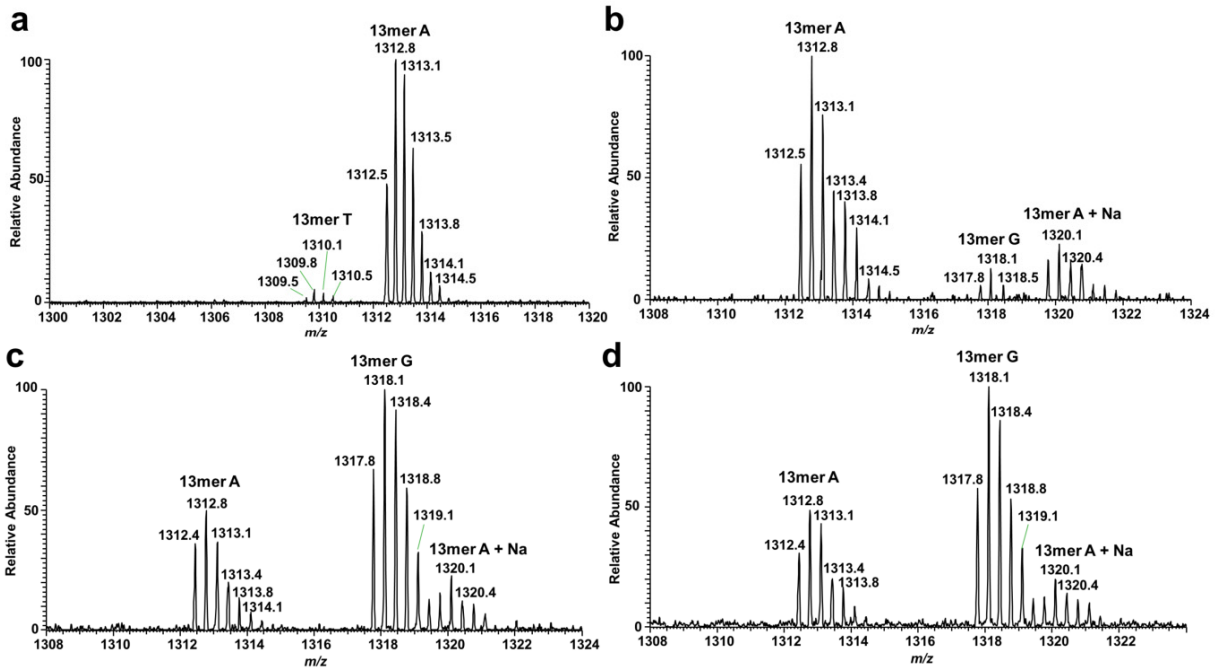

Figure S14. Representative ESI-MS/MS for monitoring the 13-mer restriction fragments of interest with A→U, A→G or A→C mutation opposite the original lesion sites. Shown are the MS/MS for monitoring the fragmentations of the $[M–3H]^{3–}$ ions of (a) (AATTATAGCACGC) (non-mutagenic product, *m/z* 1312.8), (b) d(AATTATAGCTCGC) (A→U mutation, *m/z* 1309.8), (c) d(AATTATAGCGCGC) (A→G mutation, *m/z* 1318.1), and (d) d(AATTATAGCCCGC) (A→C mutation, *m/z* 1304.8), respectively.

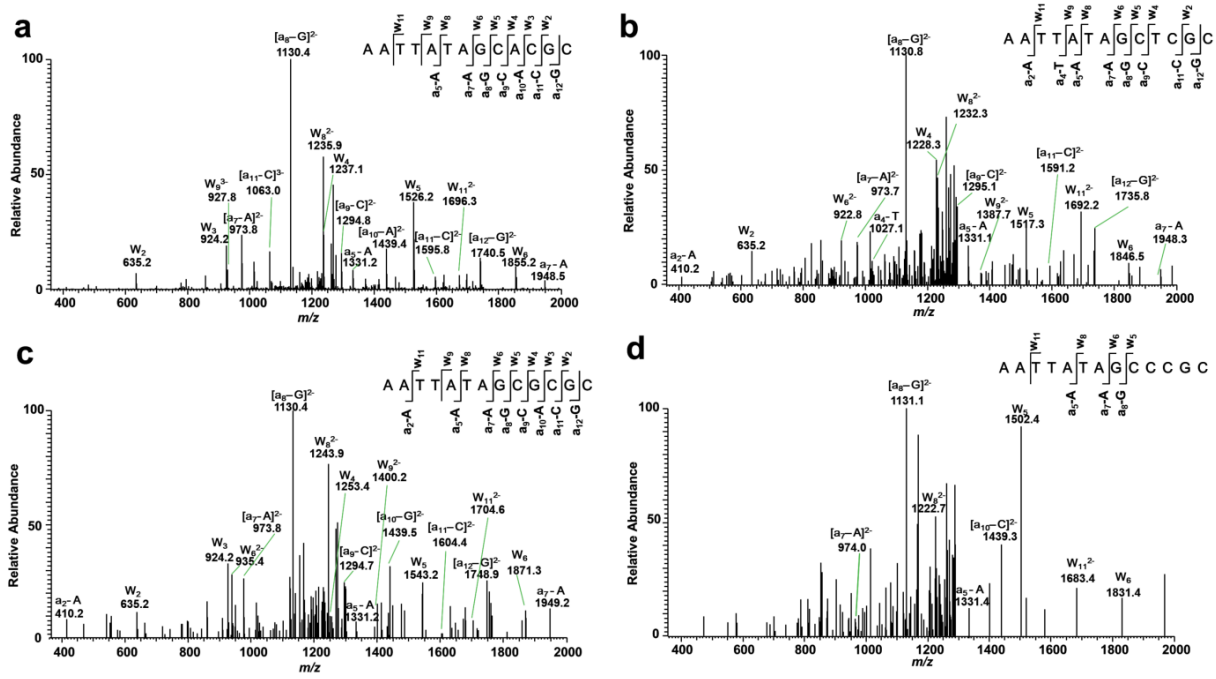

Figure S15. Restriction digestion and post-labeling method for determining the bypass efficiencies and mutation frequencies of O^2-*n*BudT, O^4-*n*BudT and O^4-POBdT in HeLa cells. (a) Representative gel image showing the NcoI/SfaNI-treated restriction fragments of interest. '16mer-comp' represents the standard ODN d(CATGGCGATATGCTAT), which corresponds to the restriction fragment arising from the competitor vector; '13mer-C', '13mer-A', '13mer-G' and '13mer-T' represent the standard ODN d(CATGGCGNGCTAT), where 'N' is C, A, G, T, respectively. (b) Representative gel image showing the MluCI/Cac8I-treated restriction fragments of interest. '10mer-C', '10mer-A', '10mer-G' and '10mer-T' represent the standard ODN d(AATTATAGCM), where 'M' is C, A, G, T, respectively.

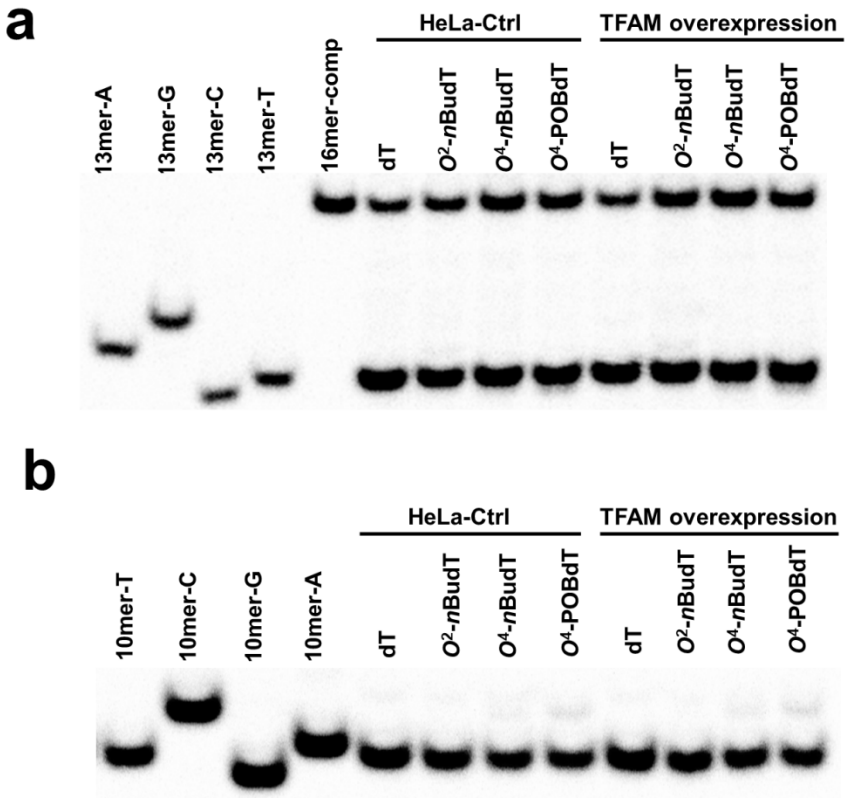

Figure S16. Representative ESI-MS results showing the detection of the $[M-3H]^{3-}$ ions of restriction fragments of interest arising from *in vivo* transcription of O^2-*n*BudT- (a), O^4-*n*BudT- (b) or O^4-POBdT-bearing substrates (c). '13mer A' represents the non-mutagenic product, i.e., d(AATTATAGCACGC), whereas '13mer T' and '13mer G' designate the corresponding products carrying an A→U, A→C or A→G mutation opposite the lesion site, i.e., d(AATTATAGCTCGC), d(AATTATAGCCCGC) and d(AATTATAGCGCGC), respectively.